Carcinogenesis vol.35 no.9 pp.1951–1961, 2014
doi:10.1093/carcin/bgu049
Advance Access publication February 22, 2014

Combination of AKT inhibition with autophagy blockade effectively reduces ascites-derived ovarian cancer cell viability

Rohann J.M.Correa[1,2], Yudith Ramos Valdes[1], Teresa M.Peart[1,3], Elena N.Fazio[1], Monique Bertrand[1,4], Jacob McGee[1,4], Michel Préfontaine[1,4], Akira Sugimoto[1,4], Gabriel E.DiMattia[1,2,4,5,†], Trevor G.Shepherd[1,3,4,5,*,†]

[1]Translational Ovarian Cancer Research Program, London Regional Cancer Program, London, Ontario, N6A 4L6, Canada, [2]Department of Biochemistry and [3]Department of Anatomy and Cell Biology, University of Western Ontario, London, Ontario, N6A 5C1, Canada, [4]Department of Obstetrics and Gynaecology, University of Western Ontario, London, Ontario, N6A 5W9, Canada and [5]Department of Oncology, University of Western Ontario, London, Ontario, N6A 4L6, Canada

*To whom correspondence should be addressed. Tel: +1 519 685 8500 56347; Fax: +1 519 685 8673;
Email: tshephe6@uwo.ca

Recent genomics analysis of the high-grade serous subtype of epithelial ovarian cancer (EOC) show aberrations in the phosphatidylinositol 3-kinase (PI3K)/AKT pathway that result in upregulated signaling activity. Thus, the PI3K/AKT pathway represents a potential therapeutic target for aggressive high-grade EOC. We previously demonstrated that treatment of malignant ascites-derived primary human EOC cells and ovarian cancer cell lines with the allosteric AKT inhibitor Akti-1/2 induces a dormancy-like cytostatic response but does not reduce cell viability. In this report, we show that allosteric AKT inhibition in these cells induces cytoprotective autophagy. Inhibition of autophagy using chloroquine (CQ) alone or in combination with Akti-1/2 leads to a significant decrease in viable cell number. In fact, Akti-1/2 sensitizes EOC cells to CQ-induced cell death by exhibiting markedly reduced EC50 values in combination-treated cells compared with CQ alone. In addition, we evaluated the effects of the novel *s*pecific and *p*otent *aut*ophagy *in*hibitor-*1* (Spautin-1) and demonstrate that Spautin-1 inhibits autophagy in a Beclin-1-independent manner in primary EOC cells and cell lines. Multicellular EOC spheroids are highly sensitive to Akti-1/2 and CQ/Spautin-1 cotreatments, but resistant to each agent alone. Indeed, combination index analysis revealed strong synergy between Akti-1/2 and Spautin-1 when both agents were used to affect cell viability; Akti-1/2 and CQ cotreatment also displayed synergy in most samples. Taken together, we propose that combination AKT inhibition and autophagy blockade would prove efficacious to reduce residual EOC cells for supplying ovarian cancer recurrence.

Introduction

The need for new and more effective therapeutics in ovarian cancer is highlighted by the low rate of survival experienced by patients with this disease. For women with localized disease who are treated surgically, 5-year survival is >90% (1). The vast majority of patients, however, present with metastatic disease characterized by widespread intraperitoneal dissemination (1). Although debulking surgery and chemotherapy can be initially effective at reducing tumor burden in these patients (2), advanced-stage epithelial ovarian cancer (EOC) has a high rate of disease recurrence and, as a consequence, a dramatically reduced 5-year survival rate of only 27.3% (1).

Over the last 20 years, treatment strategies for metastatic EOC have remained largely unchanged, therefore new and complementary therapeutics are needed to provide greater survival benefit to ovarian cancer patients. To this end, numerous targeted therapies are being developed and are currently undergoing clinical trials in ovarian cancer. Agents such as bevacizumab and olaparib that exploit alterations in angiogenesis and DNA damage responses pathways, respectively, have both demonstrated promising improvements in progression-free survival (3–5). Inhibitors of PI3K/AKT/mammalian target of rapamycin (mTOR) signaling are also being pursued since this pathway exhibits activating alterations in a large proportion of high-grade serous ovarian tumors (6,7). Clinical trials of such agents, however, have proved disappointing thus far in ovarian cancer. For example, inhibition of epidermal growth factor receptor family members epidermal growth factor receptor and ErbB2/HER2 have yielded overall response rates of only 0–7% (8–10). Likewise, a phase II trial of the mTORC1 inhibitor temsirolimus showed insufficient benefit in progression-free survival to warrant subsequent phase III study (11). The failure of such agents in ovarian cancer is probably a complex phenomenon attributable to many factors; we hypothesize that one key factor is the cellular survival mechanism known as autophagy.

Macroautophagy (herein referred to as autophagy) is a conserved self-digestion mechanism that functions at basal levels in eukaryotic cells to maintain homeostasis and promote survival under conditions of cellular stress (12–14). Autophagy can also be induced by numerous anticancer agents, especially those that target the PI3K/AKT/mTOR pathway and result in the inhibition of mTORC1, the canonical autophagy repressor (15,16). Therapy-induced autophagy has been shown to promote tumor cell survival (17–19), thereby blunting the effectiveness of anticancer agents. Given that phase I/II trials of novel PI3K/AKT/mTOR pathway inhibitors are currently underway in ovarian cancer (clinicaltrials.gov), it is essential to determine whether tumor cells subjected to this class of inhibitors upregulate autophagy as a cytoprotective response. If this is the case, a novel therapeutic strategy may involve combining PI3K/AKT/mTOR pathway inhibitors with autophagy inhibitors to minimize the tumor cytoprotective response and maximize therapeutic efficacy.

Our studies focused on metastatic high-grade serous ovarian cancer, utilizing cell cultures derived from patient ascites (fluid in the peritoneal cavity that accumulates as a result of metastatic disease) (20). Ascites contains single tumor cells and multicellular aggregates or spheroids (21–23), the dissemination of which throughout the peritoneal cavity is thought to seed secondary metastases (21,22,24,25). Thus, we utilized both non-adherent spheroid cultures and traditional adherent monolayers in our studies. We demonstrate that although AKT inhibition reduced the proliferation of these cells in a dose- and time-dependent manner, it also robustly induced autophagy. When autophagic flux was blocked pharmacologically using the classical autophagy inhibitor chloroquine (CQ) or the novel *s*pecific and *p*otent *aut*ophagy *in*hibitor-*1* (Spautin-1), cell viability was significantly reduced in both adherent and spheroid cultures. Furthermore, combined AKT inhibition and autophagy blockade acted synergistically to impair cell survival. These results indicate that when faced with pharmacologic inhibition of PI3K/AKT/mTOR signaling, ascites-derived ovarian cancer cells use the conserved process of autophagy as a prosurvival mechanism.

Materials and methods

Culture of ovarian cancer cell lines and ascites-derived cells

All work with patient materials has been approved by University of Western Ontario Health Sciences Research Ethics Board (Protocol # 12668E and 16391E). Primary cultures of ascites cells were established as described

Abbreviations: CI, combination index; CQ, chloroquine; DMSO, dimethyl sulphoxide, EOC, epithelial ovarian cancer; GFP, green fluorescent protein; PBS, phosphate-buffered saline.

[†]These authors contributed equally to this work.

previously (26) with the majority of patients diagnosed with advanced stage (II–IV), high-grade serous EOC (Supplementary Table S1, available at *Carcinogenesis* Online). The iOvCa147-E2 cell line was derived from the EOC147 ascites sample. Established cell lines were purchased from the American-Type Culture Collection (Manassas, VA) and cultured in Dulbecco's Modified Eagle Medium (HeLa), RPMI-1640 (OVCAR8, HEY, HEYA8) or alpha modified Eagle medium (OVCA429; Wisent, St. Bruno, Canada) supplemented with 5% fetal bovine serum (Wisent). To establish OVCAR8 eGFP-LC3B cells, the pBMN-ires-puro-eGFP-LC3B vector (gift from Dr C.McCormick, Dalhousie University) was transfected into OVCAR8 cells followed by selection using puromycin (1 μg/ml). Clones with robust green fluorescent protein (GFP) expression and starvation-induced punctae formation were chosen for experiments.

Adherent cells were maintained on tissue-culture-treated polystyrene (Sarstedt, Newton, NC). Non-adherent cells were maintained on ultra-low attachment cultureware (Corning, NY), which is coated with a hydrophilic, neutrally charged hydrogel to prevent cell attachment.

Cell viability assays

Adherent culture. Cells were seeded to 96-well flat-bottom tissue culture plates (EOCs: 2500–5000/well; iOvCa147-E2 5000/well) and treatments initiated the next day. At indicated time points, alamarBlue reagent (Invitrogen, Carlsbad, CA) was mixed with fresh complete medium according to manufacturer's instructions and added to each well. To perform apoptosis assays, Caspase-Glo 3/7 reagent (Promega, Madison, WI) was used as per manufacturer's instructions. Using a microplate spectrophotometer (Wallac 1420 Victor 2; PerkinElmer, Waltham, MA), fluorescence was detected for alamarBlue assays (excitation, 560 nm; emission, 590 nm) or transferred to a white-walled 96-well microplate to measure luminescence for Caspase-Glo 3/7 assays. Treatments were conducted in at least triplicate wells and readings normalized to cells treated with vehicle control.

Spheroid culture. Cells were seeded to 24-well ultra-low attachment plates at a density of 5.0×10^4 per well to form spheroids as described previously (21) and treatment was initiated at time of seeding. At 72 h post-treatment, spheroids were collected, pelleted and briefly loosened/disaggregated by trypsinization (~5 min). CellTiter-Glo reagent (Promega, Madison, WI) was prepared according to manufacturer's instructions and added to spheroids in trypsin (1:1 volume ratio). Approximately 200 μl of the mixture was added to a white-walled 96-well microplate and luminescence signal was detected using a microplate spectrophotometer (Wallac 1420 Victor 2; PerkinElmer, Waltham, MA). Treatments were conducted in at least triplicate wells and luminescence readings normalized to cells treated with vehicle control.

Immunoblotting, antibodies and other reagents

Whole-cell protein lysates were obtained and immunoblots performed as described previously (21). Antibodies against p-Akt-Ser473 (#9271), Akt (#9272S), LC3B (#2775) and Beclin-1 (#3738S) were obtained from Cell Signaling Technology (Danvers, MA). Anti-Actin antibody (A 2066) and chloroquine (C-6628) were obtained from Sigma (St. Lewis, MO). Akt inhibitor VIII (Akti-1/2) was purchased from EMD/Calbiochem (#12408; San Diego, CA). Spautin-1 was obtained from Cellagen Technology (#C3430-2s; San Diego, CA).

Immunofluorescence

Analysis of LC3 protein localization by immunofluorescent staining was performed on cells seeded to glass coverslips and treated with Akti-1/2 or dimethyl sulphoxide (DMSO) vehicle control for 24 h. Cells were fixed in a buffered 10% formalin solution, washed with phosphate-buffered saline (PBS) and permeabilized with 0.1% Triton X-100 in PBS. Overnight incubation with anti-LC3 primary antibody (1:250) was followed by anti-rabbit fluorescein isothiocyanate-conjugated secondary antibody (1:250; Vector Laboratories) and staining with 4′,6-diamidino-2-phenylindole (1:5000; Sigma, St. Louis, MO). Fluorescence images of mounted coverslips (VectaShield mounting medium; Vector Laboratories) were captured using an Olympus AX70 upright microscope and ImagePro software.

Transmission electron microscopy

Adherent primary EOC cells treated with Akti-1/2 or vehicle control for 24 h were harvested in cold fixative (2.5% glutaraldehyde in PBS pH 7.2–7.4), incubated for 16 h, then extensively washed in PBS. Samples were incubated for 1 h in 1% osmium tetroxide in buffer, embedded in 2% agarose plugs, then dehydrated in a graded series of acetone (20–100%) before transferring to liquid Epon 812 epoxy resin. Samples were poured into moulds and baked overnight prior to sectioning. At the Biotron Facility (University of Western Ontario), sections were cut on an Ultramicrotome (60 nm), picked up on copper mesh grids, and stained with uranyl acetate and lead citrate before visualization on a Phillips CM10 Transmission Electron Microscope and digital imaging.

Small interfering RNA Transfection

For RNA interference-mediated knockdown of gene expression, Dharmacon siGENOME SMARTpool reagents (Thermo Scientific, Waltham, MA), each containing a mixture of four unique small interfering RNA [siRNAs; Non-Targeting Control Pool #2 (D-001206-14-05), *BECN1* (M-010552-01), *ATG5* (M-004374-04) and *ATG7* (M-020112-01)]. Cells were seeded to 6-well plates at a density of 200 000 cells/well in antibiotic-free medium and allowed to attach overnight. The next day, siRNA and transfection reagent (DharmaFect #1, T-2001–02) were each diluted in separate tubes containing 200 ul of serum-free medium. Following 5 min incubation, siRNA-containing medium was added to DharmaFect-containing medium. This mixture was allowed to incubate for 20 min to allow liposome formation and siRNA loading. Antibiotic-free complete medium was then added to a final volume of 2 ml and plated onto cells. Transfected cells were split 1:2 48 h later into new 6-well plates and allowed to attach overnight. The next day, cells were retransfected exactly as before, so as to achieve more efficient and sustained knockdown for an extended period of time. Cells were reseeded 24 h later for subsequent experimentation.

Combination index analysis

Interaction effects of drug combinations (CQ + Akti-1/2 or Spautin-1 + Akti-1/2) were assessed using combination index (CI) and isobologram analysis, as described previously (27). EC50 values for each were determined empirically using the alamarBlue viability assay and non-linear curve-fit analysis. Based on their individual EC50s, serial dilutions of either drug alone or their combination were generated such that a 1:1 equipotent ratio was maintained at all dilutions. Viability assays were conducted as described above, and the readings analyzed using the CalcuSyn 2.0 Software (BioSoft, Cambridge, UK) to generate Isobolograms and CI scores. The isobologram is generated by plotting EC50 values for each drug as *x*- and *y*-intercepts that are connected by a line segment. As well, a single point that represents the CI score is plotted. A CI value to the left, overlapping, or to the right of the line segment indicates synergistic (CI < 1), additive (CI = 1) or antagonistic effects (CI > 1), respectively.

Graphing and statistical analysis

All graphs were generated using GraphPad Prism 5 (GraphPad Software, San Diego, CA) or Microsoft Excel 2011 (Microsoft Corporation, Redmond, WA). Data were expressed as mean ± SD or mean ± SEM, as indicated. All statistical analysis [Student's *t*-test, analysis of variance with Tukey's multiple comparison test, and non-linear curve-fit analysis to generate and compare EC50 values] was performed using GraphPad Prism 5. Tests of significance were set at $P \leq 0.05$.

Results

Allosteric AKT inhibition induces autophagy in ovarian cancer cells

The AKT kinases are a pivotal node in the PI3K/AKT/mTOR pathway, which phosphorylate numerous downstream targets to regulate cellular functions including growth, proliferation and survival (reviewed in ref. 28). The small molecule, allosteric inhibitor Akti-1/2 (or Akt Inhibitor VIII), locks the quaternary structure of AKT kinases in an inactive state, thus preventing phosphorylation and recruitment to PI3K-generated membrane phospholipids that are necessary for its activation (29).

We tested the effect of Akti-1/2 treatment on ascites-derived cancer cells from patients with high-grade serous ovarian cancer. As a measure of AKT activity, phosphorylation at Ser 473 was assessed as this modification facilitates subsequent phosphorylation at Thr 308 that is required for full kinase activation (30). Upon Akti-1/2 treatment, we observed a dose-dependent decrease in AKT phosphorylation relative to total AKT protein in the ascites-derived iOvCa147-E2 cell line and multiple EOC samples (EOC129 is depicted; Figure 1A). We also observed a dose-dependent decrease in cell viability following 72 h of Akti-1/2 treatment, quantified by the alamarBlue assay (Figure 1B), and used these data to perform non-linear curve-fit analysis and determine EC50 values (range 4.5–10.9 μM; Figure 1C). Treating ascites-derived cells with a single EC50 dose significantly decreased cell number over a 7-day period compared with vehicle-treated controls (Figure 1D). Therefore, at doses that abolish AKT serine-473 phosphorylation, we observe significant decreases in cell growth in a dose- and time-dependent manner.

The mTOR Complex 1 (mTORC1) is activated downstream of AKT and is a canonical repressor of autophagy (31). We postulated that Akti-1/2 treatment of EOC cells would reduce mTORC1 activity and, as a consequence, de-repress autophagy. Indeed, we observed

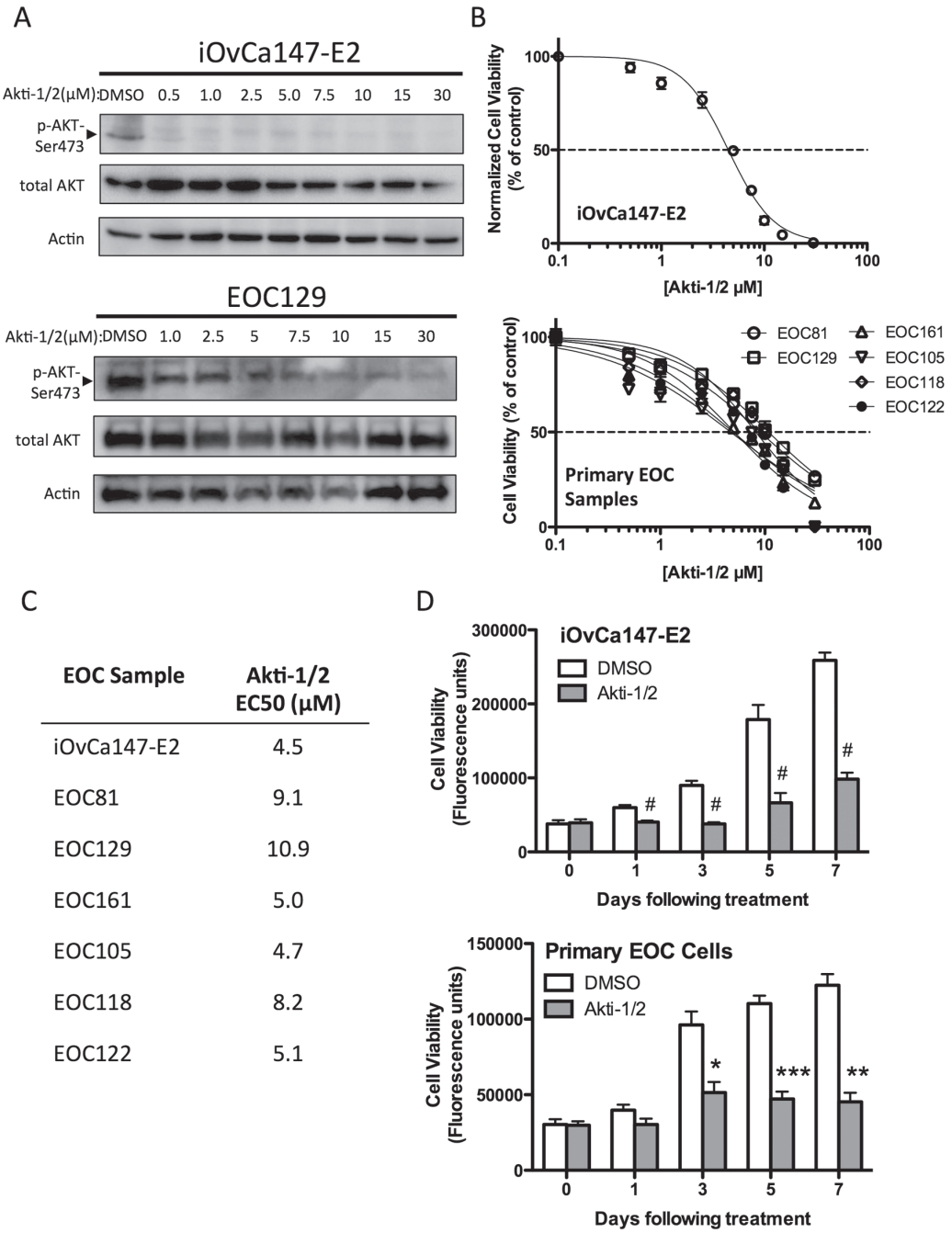

EOC Sample	Akti-1/2 EC50 (μM)
iOvCa147-E2	4.5
EOC81	9.1
EOC129	10.9
EOC161	5.0
EOC105	4.7
EOC118	8.2
EOC122	5.1

Fig. 1. Akti-1/2 inhibits AKT phosphorylation and reduces the viability of ascites-derived ovarian cancer cells. (**A**) iOvCa147-E2 cells or EOC samples were serum starved (0% fetal bovine serum) overnight, then stimulated with complete medium (10% fetal bovine serum) containing increasing [Akti-1/2] as indicated. Lysates were obtained 30 min post-treatment and immunoblot was performed for indicated proteins (representative of three experiments with iOvCa147-E2 and of five independent EOC samples). (**B**) Cell viability was assessed in iOvCa147-E2 cells ($n = 3$) and EOC samples ($n = 6$) using the alamarBlue assay at 72 h post-treatment. Non-linear curve-fit analysis was performed to generate a dose–response curve to determine the Akti-1/2 EC50 values listed in (**C**). (**D**) Cells were treated with Akti-1/2 (EC50) and viability assessed over time. Student's *t*-test was used to compare DMSO with Akti-1/2 treatment at each time point (iOvCa147-E2, $n = 3$ experiments; $n = 3$ independent EOC samples; $^{*}P \le 0.05$; $^{**}P \le 0.01$; $^{***}P \le 0.001$; $^{\#}P \le 0.0001$).

increased processing of the autophagy marker LC3 (microtubule-associated protein light chain 3; Figure 2A). The cleaved and lipidated form of this protein (LC3-II) is identifiable as a faster-migrating species and indicates the presence of autophagosomes since LC3-II is integral to their formation (32). We confirmed mTORC1 inhibition since Akti-1/2 treatment resulted in a dose-dependent decrease in phosphorylation of the direct target of mTORC1, p70 S6 Kinase (pS6K-T389; Figure 2A). Additionally, using indirect immunofluorescence, accumulation and localization of LC3 into discrete autophagosome-associated punctae was observed in Akti-1/2-treated EOC cells (Figure 2B). To confirm that the Akti-1/2-induced punctate structures were autophagosomes and autolysosomes, primary EOC cells were treated with Akti-1/2 or DMSO and prepared for transmission electron microscopic analysis. Indeed, AKT inhibition resulted in numerous autolysosomes in the cytoplasm of cells compared with vehicle-treated control cells (Figure 2C).

We also performed autophagic flux experiments to verify autophagy induction and distinguish it from late-stage inhibition. The antimalarial agent CQ is a small molecule that disrupts lysosome function by increasing intralysosomal pH. Since lysosomes

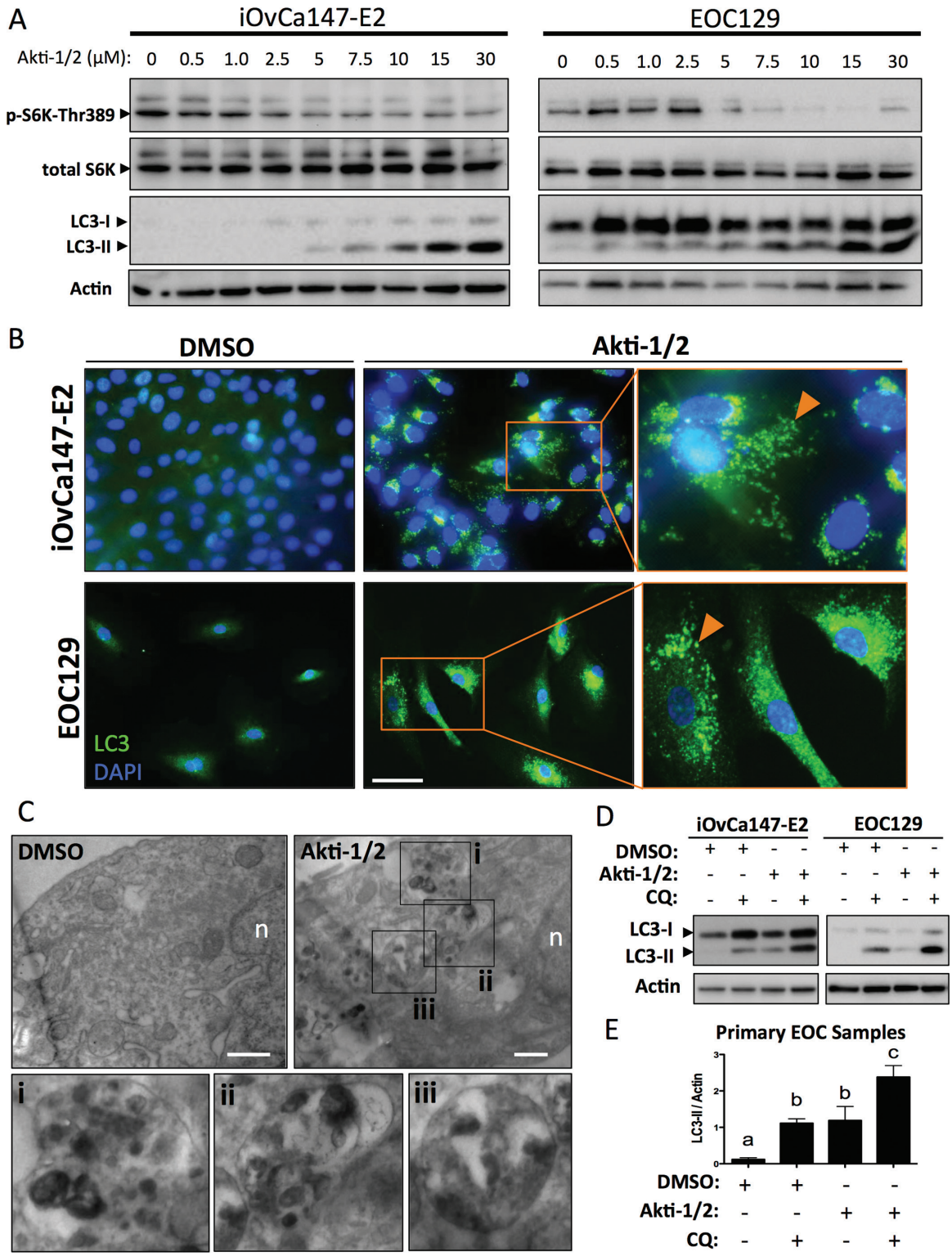

Fig. 2. Akti-1/2 upregulates autophagy in ascites-derived ovarian cancer cells. (**A**) iOvCa147-E2 or EOC samples were incubated with increasing [Akti-1/2] in complete medium (10% fetal bovine serum) for 24 h. Lysates were obtained and immunoblot was performed for indicated proteins (representative blots of three experiments with iOvCa147-E2 and of five independent EOC samples). (**B**) iOvCa147-E2 or EOC samples were seeded to glass coverslips and subsequently incubated with Akti-1/2 (20 μM) or DMSO control in complete medium (10% fetal bovine serum) for 24 h. Indirect immunofluorescence was performed using anti-LC3 antibody and nuclei were stained with 4′,6-diamidino-2-phenylindole. Scale bar, 50 μm. (**C**) Transmission electron microscopy was performed on EOC67 cells treated with Akti-1/2 or DMSO as indicated. Insets of Akti-1/2-treated cell images (i–iii) indicate autolysosome structures in the cytoplasm. Scale bar, 500 nm; n, nucleus. (**D**) Cells in 6-well plates were treated with Akti-1/2 (EC50) ± CQ (50 μM) and lysates obtained 24 h post-treatment, and immunoblot was performed for indicated proteins. Representative blots of iOvCa147-E2 and EOC129 are depicted. Quantification of LC3II expression relative to actin are shown, as determined using the Chemidoc System and ImageLab 4.1 software (Biorad). (**E**) Quantification of LC3-II was normalized to actin for five independent EOC samples and one-way analysis of variance with Tukey's multiple comparison test was used to compare means. Letters denote statistically significant differences ($P \leq 0.01$). Data are represented as mean ± SEM.

are essential for the degradation of autophagic cargo, their disruption by CQ causes accumulation of undegraded autophagosomes studded with LC3-II (33). Therefore, autophagy induction by Akti-1/2 treatment followed by administration of CQ should impair autophagosome clearance, resulting in an even greater increase in LC3-II. This was evident in EOC cells, where a short (4 h) treatment of CQ (50 μM) resulted in a buildup of LC3-II in untreated cells and an even greater accumulation in cells treated with Akti-1/2, confirming that autophagy is actively induced as a consequence of AKT inhibition (Figure 2D and E); this effect was also observed in OVCAR8 eGFP-LC3B cells with significant relocalization of GFP into punctae (Supplementary Figure S1A, available at *Carcinogenesis* Online) and increased LC3-II levels (Supplementary Figure S1B, available at *Carcinogenesis* Online).

To confirm these results obtained using CQ for autophagy blockade, we also knocked down the expression of known autophagy regulators *BECN1*, *ATG5* and *ATG7* using siRNA. Reducing ATG5 and ATG7 protein expression decreased autophagy induction by Akti-1/2, and their combined depletion blocked autophagy in iOvCa147-E2 cells even further (Figure 3A). Reduced Beclin-1 expression, however, had no effect on Akti-1/2-mediated autophagy induction. Knockdown of both *ATG5* and *ATG7* correlated with decreased cell viability over time (Figure 3B), thus confirming our findings that autophagy upregulation serves a prosurvival function in ascites-derived ovarian cancer cells.

AKT inhibition combined with chloroquine-mediated autophagy blockade reduces ovarian cancer cell viability

Given that autophagy upregulation may be acting as a potential survival response to AKT/mTORC1 inhibition, we sought to determine the effect of blocking autophagic flux on ovarian cancer cell viability. Ascites-derived EOC cells were treated with Akti-1/2 (using individual sample EC50 values), CQ (50 μM) or both, and their viability assessed by alamarBlue assay. In multiple EOC samples, treatment with CQ or Akti-1/2 alone led to reductions in viable cells of 35–50%; their combination, however, yielded a more pronounced decrease in viability of 70–95% (Figure 4A). Data analysis using all eight individual EOC samples revealed that the decreases in cell viability were statistically significant ($P \leq 0.001$; Figure 4B). Similar results were also obtained from identical experiments using the iOvCa147-E2 cell line ($P \leq 0.001$; Figure 4C). Therefore, CQ-mediated autophagy blockade, on its own or in combination with AKT inhibition, significantly decreases cell viability. To assess whether cell death was occurring by apoptosis, we performed Caspase-Glo assays on iOvCa147-E2 and primary EOC cells treated with Akti-1/2 (10 μM), CQ (50 μM) or both. After 24 h of treatment, apoptosis activity was significantly increased in cells treated with Akti-1/2 and CQ combined; we also observed elevated apoptosis in iOvCa147-E2 cells due to Akti-1/2 treatment alone (Supplementary Figure S2A, available at *Carcinogenesis* Online).

Although LC3-II accumulation upon CQ treatment (Figure 2D and E) implies that autophagic flux is being blocked, the completeness and effectiveness of autophagy inhibition using a single dose of CQ cannot be inferred from increases in LC3-II alone. Thus, we opted to assess cell viability across a range of CQ concentrations. CQ was titrated in the presence of vehicle control (DMSO + CQ) to test the effect of blocking basal autophagy, or in combination with fixed-dose AKT inhibition (Akti-1/2 + CQ) to test the effect on blocking induced autophagy. Using iOvCa147-E2 cells, comparison of cells treated with DMSO or Akti-1/2 revealed a significant difference in CQ EC50s. Specifically, Akti-1/2 cotreatment caused a 67% decrease in CQ EC50 from 68.4 μM to 22.7 μM, suggesting that AKT inhibition sensitized these cells to CQ-mediated autophagy blockade (Figure 4D). Ascites-derived EOC cells exhibited a broad range of sensitivity to CQ alone (EC50s of 25 μM–150 μM), which was significantly decreased by 32–78% in the presence of Akti-1/2 (Figure 4E). Taken together, these findings demonstrate that AKT inhibition sensitizes metastatic ovarian cancer cells to the deleterious effects of autophagy blockade.

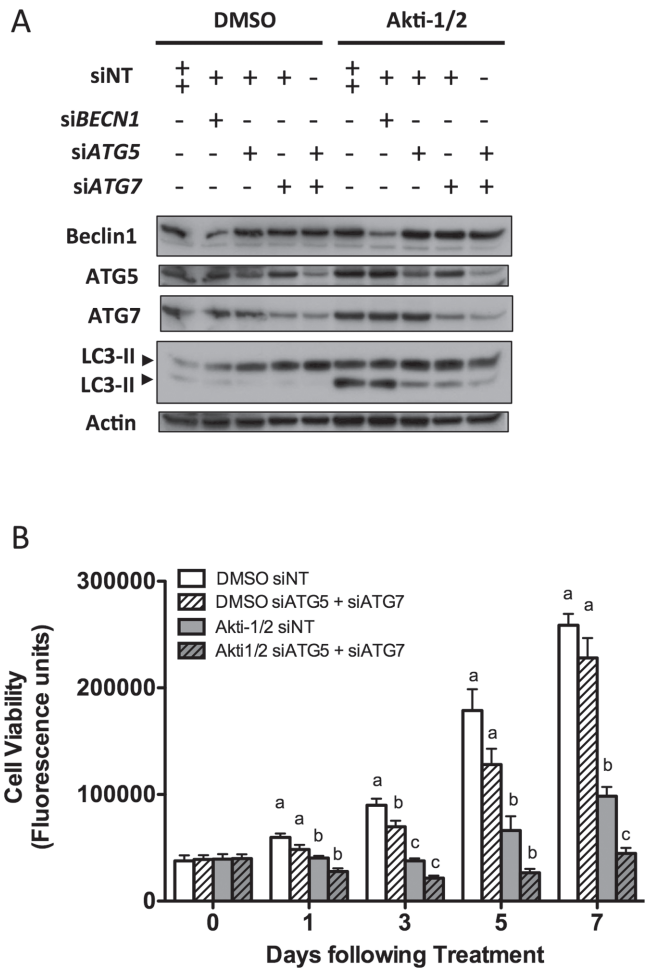

Fig. 3. RNA interference-mediated autophagy blockade reduces the viability of ascites-derived ovarian cancer cells. The iOvCa147-E2 cell line was transfected with non-targeting siRNAs (siNT) or siRNA pools targeting *BECN1*, *ATG5* and *ATG7*. Transfection was repeated 72 h later, and following overnight incubation, cells were seeded for subsequent experiments. (**A**) At 10 days after initial transfection, iOvCa147-E2 cells were treated for 24 h with either DMSO or Akti-1/2 (3.5 μM). Lysates were obtained and immunoblots performed for indicated proteins. Blot represents four repeated experiments. (**B**) At 5 days post-transfection, cells were treated with DMSO vehicle control or Akti-1/2 (3.5 μM) in quadruplicate and viability assessed by alamarBlue assay at indicated time points. Data are pooled from three experiments and represented as mean ± SEM.

Autophagy blockade mediated by the specific and potent autophagy inhibitor 1 (Spautin-1) reduces the viability of ovarian cancer cells subjected to AKT inhibition

Spautin-1 was the first targeted autophagy inhibitor to be published (34). It is a small molecule that inhibits USP10 and USP13, two ubiquitin-specific peptidases responsible for stabilizing members of the autophagy-inducing class III PI3K (PI3K C3) complex. By inhibiting USP10/13, Spautin-1 has been reported to cause the degradation of multiple complex members (Beclin-1, ATG14L, p150 and PI3K C3), in turn blocking autophagy induction.

We tested Spautin-1 in ascites-derived EOC cells and demonstrated that it can effectively block autophagy upregulation by Akti-1/2. In iOvCa147-E2 cells and primary EOC samples cotreated with Akti-1/2 and Spautin-1, LC3-II expression was reduced, and to near-basal levels in the case of primary EOC cells (Figure 5A). Densitometry of LC3 immunoblots revealed this reduction to be significant across all EOC samples tested (Figure 5B). For further confirmation, Spautin-1 effectively blocked autophagosome punctae formation and

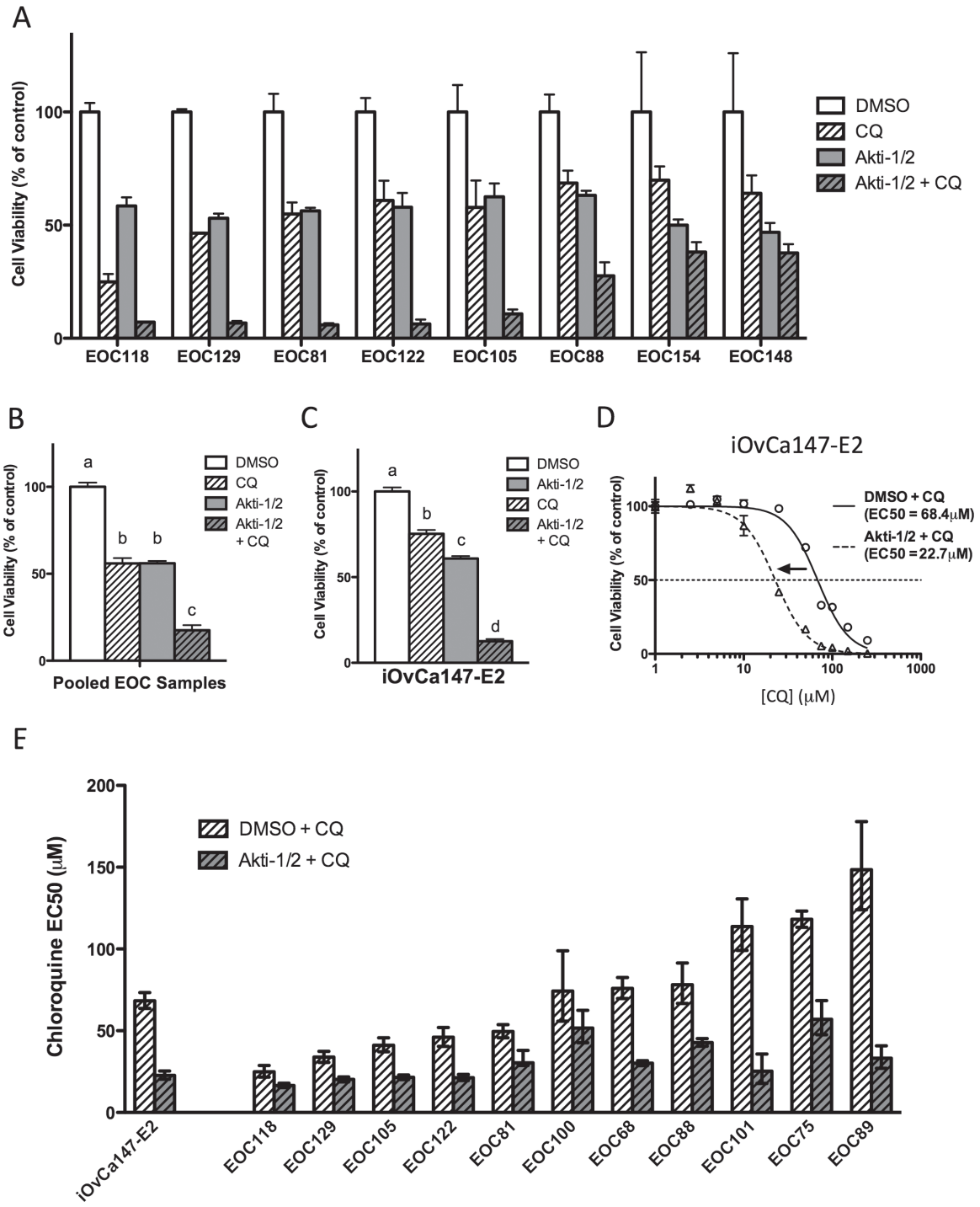

Fig. 4. AKT inhibition combined with CQ treatment reduces cell viability. (**A**–**C**) Triplicate wells of 96-well plates were seeded, allowed to attach overnight, treated for 72 h with Akti-1/2 (EC50) and CQ (50 μM), and viability assessed by alamarBlue. (A) Viability readings normalized to vehicle control (DMSO) for eight individual EOC samples. Bars: mean ± SD. (B) Normalized viability data pooled from all EOC samples ($n = 8$) and (C) iOvCa147-E2 cells ($n = 3$). Bars: mean ± SEM. Different letters denote statistically significant differences based on one-way analysis of variance with Tukey's test of multiple comparisons ($P \leq 0.001$). (**D** and **E**) Triplicate wells were treated with a range of CQ doses (0, 2.5, 5.0, 10, 25, 50, 75, 100, 150, 250 μM) combined with either DMSO or Akti-1/2 (EC50) and viability assessed at 72 h. (D) Non-linear curve-fit analysis and EC50 comparisons performed for iOvCa147-E2 cells ($P < 0.001$). (E) CQ EC50 comparisons for iOvCa147-E2 cells and 11 independent EOC samples. Bars: mean ± 95% confidence interval.

LC3-II processing in Akti-1/2-treated OVCAR8 eGFP-LC3B cells (Supplementary Figure S3, available at *Carcinogenesis* Online).

Interestingly, despite its published mechanism of action (34), Spautin-1-mediated autophagy blockade in EOC cells did not correlate with a reduction in Beclin-1 protein levels (Figure 5A and B), suggesting that Beclin-1 was not critical for Spautin-1's mechanism of action in our system. This may be a common feature of ovarian cancer cells, since we made similar observations in established ovarian cancer cell lines OVCA429, HEY and HEYA8 (Supplementary Figure S4A, available at *Carcinogenesis* Online). In contrast, HeLa cervical carcinoma cells exhibit reduced Beclin-1 levels upon Akti-1/2 and Spautin-1 cotreatment (Supplementary Figure S4B, available at *Carcinogenesis* Online), in agreement with the original characterization of Spautin-1 by Liu *et al.* (34). To further test the contribution

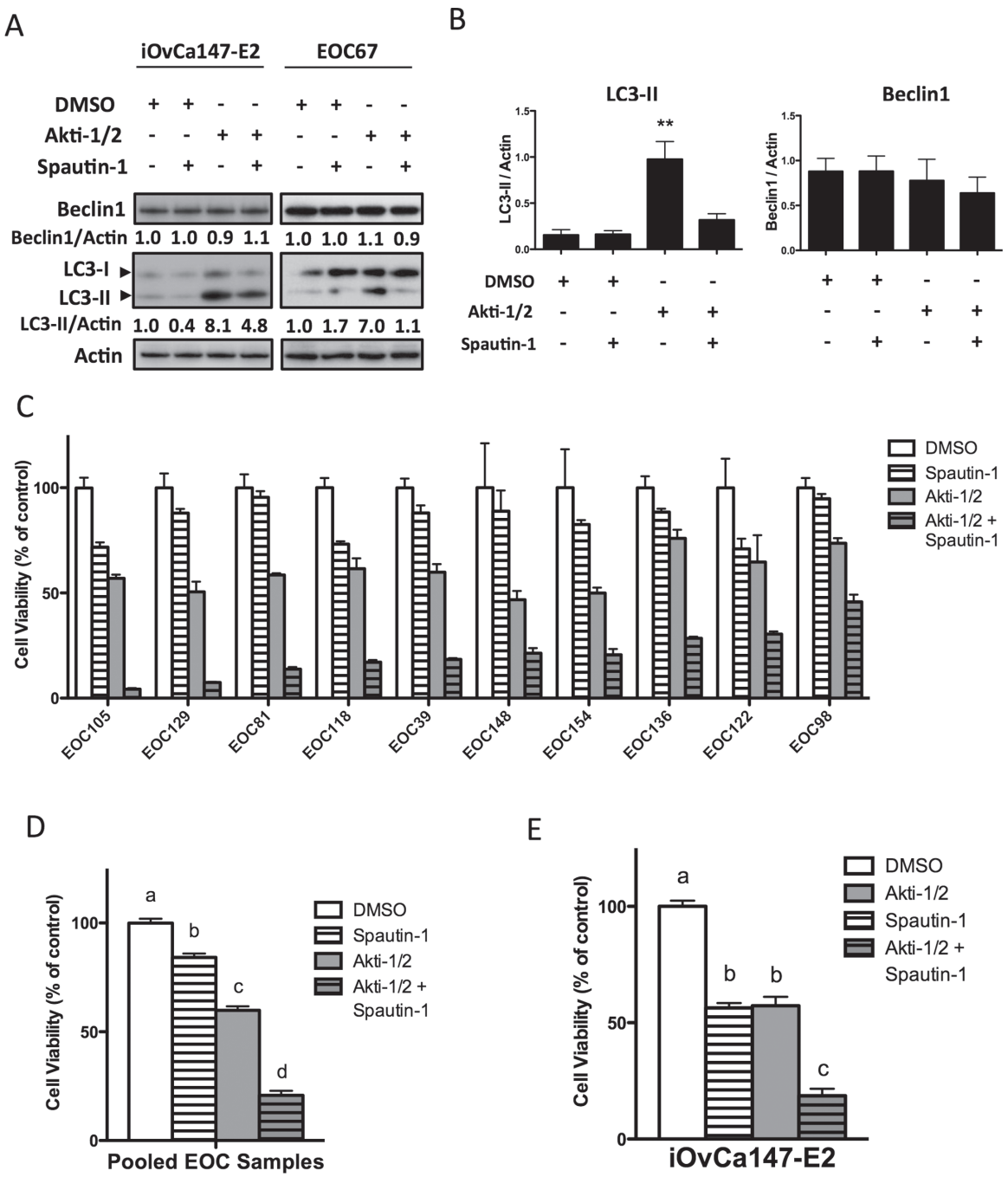

Fig. 5. Spautin-1 blocks autophagy upregulation and reduces ovarian cancer cell viability. (**A**, **B**) Cells in 6-well plates were treated with Akti-1/2 (EC50) ± Spautin-1 (10 μM) and lysates obtained 24 h post-treatment, and immunoblot were performed for indicated proteins. (A) Representative blots of iOvCa147-E2 and EOC67 cells are depicted. Quantification of Beclin-1 and LC3II expression relative to actin are shown, as determined using the Chemidoc System and ImageLab 4.1 software (Biorad). (B) Quantification of band intensity of LC3-II or Beclin-1 normalized to Actin ($n = 5$ independent EOC samples). Data are represented as mean ± SEM. One-way analysis of variance with Tukey's multiple comparison test compared means (**$P \leq 0.01$). (**C**–**E**) For viability assays, triplicate wells were seeded to 96-well adherent plates and treated following overnight incubation (Akti-1/2 EC50, Spautin-1 10 μM). Viability was assessed by alamarBlue assay at 72 h. (C) Viability readings were normalized to DMSO vehicle control. Bars: mean ± SD. (D) Data from 10 EOC samples were pooled and one-way analysis of variance with Tukey's multiple comparison test performed. (E) iOvCa147-E2 cells were treated and analyzed identically ($n = 3$ experiments). Data are represented as mean ± SEM. Different letters denote statistically significant differences among treatments ($P \leq 0.001$).

of Beclin-1 to Spautin-1-mediated autophagy blockade, we also compared its effect on Beclin-1-expressing and Beclin-1-depleted cells. We found that comparable autophagy blockade was achieved by Spautin-1 even when Beclin-1 expression was knocked down by siRNA transfection of iOvCa147-E2 cells (Supplementary Figure S4C, available at *Carcinogenesis* Online). These data demonstrate that Spautin-1 efficiently blocks Akti-1/2-mediated autophagy upregulation in EOC cells and that this occurs in a Beclin-1-independent manner.

Given that Spautin-1 efficiently inhibited Akti-1/2-mediated autophagy upregulation, we then asked what effect simultaneous treatment with Akti-1/2 and Spautin-1 would have on cell viability. Treatment with single-agent Spautin-1 (10 μM) had a modest effect on all EOC samples tested, resulting in no greater than a 30% loss of viability, whereas single-agent Akti-1/2 (EC50) yielded the expected 50% decrease. When cells were treated with both agents, however, a decrease in viability of ≥75% was observed in all EOC samples

(Figure 5C), which was statistically significant when analyzing pooled EOC samples ($P \leq 0.001$; Figure 5D). Identical experiments were conducted with the iOvCa147-E2 cell line, revealing again that combination treatment reduced cell viability significantly more than either agent alone ($P \leq 0.001$; Figure 5E). As assessed using Caspase-Glo 3/7 activity, the combined treatment of iOvCa147-E2 and primary EOC cells with Spautin-1 and Akti-1/2 resulted in significantly increased apoptosis-mediated cell death (Supplementary Figure S2B, available at *Carcinogenesis* Online).

Spheroids are more resistant to single-agent treatment than adherent cells but remain highly sensitive to the combination of AKT inhibition and autophagy blockade

Since multicellular spheroids are considered a key aspect of the ovarian cancer metastatic process (21,22,24,25,35), we sought to determine whether these structures also responded to AKT inhibition by upregulating cytoprotective autophagy. To test this, we generated *in vitro* spheroids and subjected them to Akti-1/2 treatment. Similar to adherent cells, AKT inhibition induced autophagy

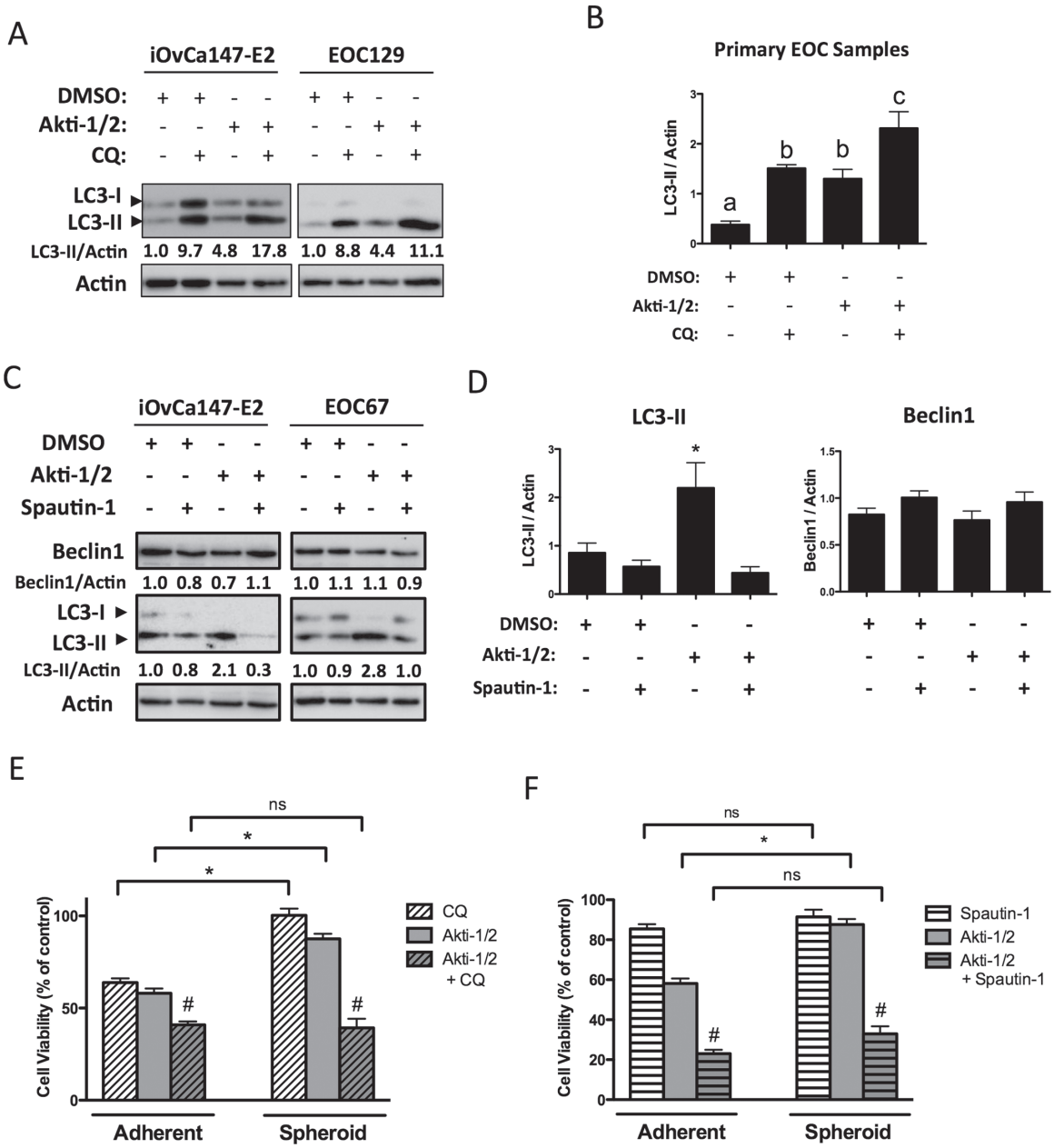

Fig. 6. Spheroids are more sensitive to combined AKT and autophagy inhibition than either treatment alone. Non-adherent cells in 6-well ultra-low attachment plates were treated (Akti-1/2 5 μM, CQ 50 μM, Spautin-1 10 μM) at time of seeding and lysates obtained 24 h post-treatment, and immunoblot was performed for indicated proteins. (**A** and **C**) Representative blots of iOvCa147-E2 and EOC129 cells (A) or iOvCa147-E2 and EOC67 cells are depicted. Quantification of Beclin-1 and LC3II expression relative to actin is shown, as determined using the Chemidoc System and ImageLab 4.1 software (Biorad). (**B** and **D**) Quantification of band intensity of LC3-II or Beclin-1 normalized to actin for multiple EOC samples ($n = 4$ or 5). Data are represented as mean ± SEM. One-way analysis of variance with Tukey's multiple comparison test compared means. Letters denote statistical significance (panel B, $P \leq 0.05$; panel D, $^{*}P \leq 0.01$). (**E** and **F**) For viability assays, cells were seeded to parallel adherent or spheroid cultures, then treated following overnight incubation or at time of seeding, respectively. Viability was quantified by and normalized to DMSO vehicle control (set to 100%). Normalized viability data from individual EOC samples ($n = 7$) treated with (E) Akti-1/2 (EC50) ± CQ (25 μM) or (F) Akti-1/2 (EC50) ± Spautin-1 (10 μM) were pooled and one-way analysis of variance with Tukey's multiple comparison test performed ($^{*}P \leq 0.001$). Drug combination more effectively decreased viability compared with single-agent treatments ($^{\#}P \leq 0.01$). Data are represented as mean ± SEM.

in spheroids, which was blocked by the coadministration of CQ (Figure 6A and B). Likewise, coadministration of Spautin-1 inhibited autophagy in spheroids, with reductions in LC3-II to below basal levels. As in adherent cells, this occurred without a change in Beclin-1 protein expression (Figure 6C and D). To assess spheroid cell viability in response to AKT and autophagy inhibition, parallel adherent and spheroid cultures were treated with EC50 doses of Akti-1/2 alone, an autophagy inhibitor alone (CQ or Spautin-1) or their combination. Spheroid cells were dramatically less sensitive to Akti-1/2, exhibiting only a 10% reduction in viable cell number compared with 50% in adherent cells ($*P \leq 0.001$; Figure 6E and F). Similarly, single-agent CQ was significantly less potent in spheroids compared with adherent cells ($*P \leq 0.001$; Figure 6E), whereas Spautin-1 treatment alone had no effect in either culture condition ($P > 0.05$; Figure 6F). Despite their attenuated response to single-agent treatment, spheroid cells remained highly sensitive to cotreatment as Akti-1/2 + CQ or Akti-1/2 + Spautin-1 was equally effective in reducing cell viability in EOC spheroids as in adherent cells ($\#P \leq 0.001$; Figure 6E and F). Taken together, these data imply that although spheroids are able to resist the effects of either AKT inhibition or autophagy blockade alone, their combination yields dramatic reductions in cell viability.

Combined AKT and autophagy inhibition act synergistically to reduce ovarian cancer cell viability

Thus far, we have demonstrated that cotreatment of ovarian cancer cells with AKT inhibition and autophagy blockade reduces cell viability to a greater extent than either alone. However, it remained to be determined whether these treatments were acting merely in an additive or synergistic manner. Synergy is valued over an additive effect since either agent can be used at lower doses (thus reducing toxicity) while still achieving therapeutic efficacy. To assess synergy, we performed isobologram analysis, which provides a quantitative combination index (CI) value as a measure of drug interaction (36). Briefly, using individual agent EC50s as a starting point, serial dilutions of either drug alone and their combination were generated with a 1:1 ratio of equipotency at all dilutions. Cell viability data were determined for each condition and CI analysis performed using these data. A CI score <1, 1 or >1 indicates synergistic, additive or antagonistic effects, respectively. For all EOC samples tested, the combination of Akti-1/2 and Spautin-1 was found to be synergistic (Table I). Synergy was also observed for the Akti-1/2 and CQ combination (in all EOC samples but one), albeit to a lesser extent than Akti-1/2 + Spautin-1. CI analyses were also performed in iOvCa147-E2 cells, revealing a synergistic and additive effect of Spautin-1 and CQ, respectively, in combination with Akti-1/2. The greater level of synergism achieved with Spautin-1/Akti-1/2 cotreatment is not unexpected since Spautin-1 treatment alone yields little effect on EOC cell viability (Figure 4C–E), whereas CQ as a single agent resulted in significant reductions in cell viability (Figure 3). In conclusion, combination treatment with AKT inhibition and autophagy blockade synergistically reduces the viability of metastatic ovarian cancer cells derived from patient ascites.

Discussion

Combinatorial autophagy blockade is an emerging paradigm in cancer treatment, providing a means of sensitizing tumor cells to existing or investigational therapeutics (37). It is based on the premise that tumor cells upregulate autophagy to mitigate the deleterious effects of anticancer agents. Consequently, blocking therapy-induced autophagy deprives them of an important survival mechanism. Our present work demonstrates that ascites-derived ovarian cancer cells treated with an AKT inhibitor upregulate autophagy to promote their survival since combined autophagy inhibition resulted in significantly decreased cell viability. Our work therefore supports a prosurvival role for autophagy induction in this context and suggests that combinatorial autophagy blockade would be a worthwhile treatment strategy to explore clinically in ovarian cancer.

We previously demonstrated that AKT inhibition in ascites-derived ovarian cancer cells reduces proliferation by inducing G0/G1 cell cycle arrest but does not induce cell death (21). Our present findings strongly suggest that autophagy is a key ovarian tumor cell survival mechanism in the face of AKT inhibition. This notion is supported by work from Lu *et al.* (38), who demonstrated that autophagy is required for the sustained survival of dormant ovarian tumor xenografts exogenously expressing the imprinted tumor suppressor gene *DIRAS3*. Our work builds on this pioneering study by assessing the role of autophagy induced by pharmacologic AKT inhibition, a therapeutic paradigm relevant to this disease site. Moreover, we have focused on the role of autophagy in EOC metastasis by directly addressing ascites-derived cells from patients with late-stage disease. Although our data lend further support to the notion of cytoprotective autophagy in the face of AKT inhibition, the mechanistic details of this require further investigation. For instance, it remains to be seen if autophagy protects cells from apoptotic or non-apoptotic cell death, as this has been demonstrated in other systems (15,18,39), and under what conditions within solid primary and secondary tumors autophagy is regulated and required. Such investigations should give way to a clearer understanding of the precise functions of autophagy in ovarian tumor growth and spread.

This study assessed the role of autophagy upregulation not only in adherent cultures but also in multicellular aggregates or spheroids as these are considered important in promoting ovarian cancer metastasis (21–25). Autophagy inhibition by CQ was significantly less efficacious in spheroids compared with adherent cells; Spautin-1 treatment was equally ineffective in both culture conditions (Figure 6E and F). We suspect that these results are attributable to the general drug-resistant phenotype inherent to EOC spheroids (reviewed in ref. 40) rather than a specific insensitivity to autophagy blockade. Indeed, it is well established that three-dimensional or "tumor-sphere" culture of ovarian cancer cells endows them with resistance to chemotherapeutics (41–45). Likewise, our findings also demonstrate reduced sensitivity to single-agent Akti-1/2 in spheroids (Figure 6E and F). Nonetheless, it is clear that modulating autophagy in spheroid cells has real potential to decrease ovarian tumor cell survival since despite apparent resistance to single-agent treatment, combining AKT inhibition and autophagy blockade achieves significant reductions in cell viability.

Table I. The combination of AKT inhibition and autophagy blockade synergistically reduces cell viability of metastatic ovarian cancer cells

Sample	Spautin-1 + Akti-1/2		Sample	Chloroquine + Akti-1/2	
	CI value	Description		CI value	Description
iOvCa147-E2	0.63	Synergy	iOvCa147-E2	1.04	Additive
EOC154	0.50	Synergy	EOC148	1.05	Additive
EOC148	0.41	Synergy	EOC154	0.84	Slight synergy
EOC129	0.27	Synergy	EOC129	0.72	Moderate synergy
EOC122	0.23	Strong synergy	EOC81	0.59	Synergy
EOC105	0.22	Strong synergy	EOC118	0.56	Synergy
EOC81	0.16	Strong synergy	EOC105	0.39	Synergy
EOC118	0.11	Strong synergy	EOC122	0.36	Synergy

As a clinical agent, CQ has been used as an antimalarial for decades and is well-tolerated with minimal toxicity in patients. CQ, or its derivative hydroxy-CQ, is being tested clinically as an autophagy inhibitor in combination with targeted anticancer agents (clinicaltrials.gov). For example, although trials of mTOR inhibitor temsirolimus have demonstrated a 0% stable disease rate in patients with metastatic melanoma, its combination with hydroxy-CQ achieved stable disease in 4/5 of patients in a phase I trial (American Association for Cancer Research 2011 Abstract #4500). Likewise, two randomized controlled trials of CQ in glioblastoma multiforme revealed that its combination with standard therapy increased mean overall survival by at least 2-fold compared with standard therapy alone (46,47). As of yet, no such trials have been initiated specifically for ovarian cancer. Our findings suggest that further evaluation of autophagy blockade combined with other anticancer agents is warranted in EOC, particularly for the treatment of high-grade serous disease.

In addition to CQ, there is growing interest in developing alternative autophagy inhibitors with improved pharmacokinetic properties (e.g. Lys05, a dimeric form of CQ) (48) and alternative mechanisms of action (e.g. Spautin-1) (34). In our hands, Spautin-1 potently blocked autophagy upregulation by Akti-1/2, leading to synergistic decreases in viability in all patient-derived cultures tested. Liu *et al.* (34) determined that class III PI3K complex members, particularly the autophagy regulator ATG6/Beclin-1, are destabilized by administration of Spautin-1 and this proteasomal degradation mediates autophagy inhibition. Although autophagy blockade correlates with decreased Beclin-1 protein levels in HeLa cells (Supplementary Figure S2B, available at *Carcinogenesis* Online), we demonstrate that in all ovarian cancer cells tested, Spautin-1 efficiently inhibits autophagy in a Beclin-1-independent manner. Our findings are not without precedent since another recent report also noted that Beclin-1 levels remain unchanged despite efficient autophagy blockade by Spautin-1 (49). Most recently, inhibition of autophagy by Spautin-1 was shown to decrease the viability of ovarian cancer cell lines by selectively targeting mutant p53 protein for lysosomal degradation (50).Therefore, Spautin-1 or its derivatives have tremendous translational potential as a highly efficacious inhibitor of autophagy in metastatic ovarian cancer cells.

Overall, this report represents an important preclinical investigation into the utility of autophagy blockade combined with targeted therapies. By demonstrating the sensitivity of ascites-derived metastatic ovarian tumor cells to autophagy inhibition, our work supports the application of this therapeutic paradigm to patients with metastatic high-grade serous carcinoma, which represents the majority of ovarian cancer diagnoses. Presently, the allosteric AKT inhibitor MK-2206 (an analog of Akti-1/2) is under investigation at the phase II level in advanced ovarian, fallopian tube and peritoneal carcinomas (NCT01283035). With our results in mind, it would be important to determine whether autophagy is upregulated in tumors of treated patients as a potential predictor for recurrence and resistance. Our findings suggest that combinatorial autophagy blockade may significantly enhance the cytotoxicity of such PI3K/AKT/mTOR pathway inhibitors, providing a novel therapeutic strategy that may someday improve the survival of patients suffering from this disease.

Supplementary material

Supplementary Table S1 and Figures S1–S4 can be found at http://carcin.oxfordjournals.org/

Funding

Canadian Institutes of Health Research (OVA-94083); Canadian Cancer Society (20109).

Acknowledgements

We acknowledge the contribution by Christine Gawlik, Kay Faroni and Carrie Thornton at the London Regional Cancer Program for providing EOC sample clinical data. We are also grateful to the women with ovarian cancer who generously donated their ascites samples to support our research.

Conflict of Interest Statement: None declared.

References

1. Howlader,N. *et al.* (eds) (2013). *SEER Cancer Statistics Review, 1975–2010*. National Cancer Institute, Bethesda, MD.
2. Coleman,R.L. *et al.* (2013) Latest research and treatment of advanced-stage epithelial ovarian cancer. *Nat. Rev. Clin. Oncol.*, **10**, 211–224.
3. Ledermann,J. *et al.* (2012) Olaparib maintenance therapy in platinum-sensitive relapsed ovarian cancer. *N. Engl. J. Med.*, **366**, 1382–1392.
4. Perren,T.J. *et al.*; ICON7 Investigators. (2011) A phase 3 trial of bevacizumab in ovarian cancer. *N. Engl. J. Med.*, **365**, 2484–2496.
5. Burger,R.A. *et al.*; Gynecologic Oncology Group. (2011) Incorporation of bevacizumab in the primary treatment of ovarian cancer. *N. Engl. J. Med.*, **365**, 2473–2483.
6. Hanrahan,A.J. *et al.* (2012) Genomic complexity and AKT dependence in serous ovarian cancer. *Cancer Discov.*, **2**, 56–67.
7. TCGA. (2011) The Cancer Genome Atlas Research Network. Integrated genomic analyses of ovarian carcinoma. *Nature*, **474**, 609–615.
8. Seiden,M.V. *et al.* (2007) A phase II trial of EMD72000 (matuzumab), a humanized anti-EGFR monoclonal antibody, in patients with platinum-resistant ovarian and primary peritoneal malignancies. *Gynecol. Oncol.*, **104**, 727–731.
9. Bookman,M.A. *et al.* (2003) Evaluation of monoclonal humanized anti-HER2 antibody, trastuzumab, in patients with recurrent or refractory ovarian or primary peritoneal carcinoma with overexpression of HER2: a phase II trial of the Gynecologic Oncology Group. *J. Clin. Oncol.*, **21**, 283–290.
10. Schilder,R.J. *et al.* (2009) Phase II trial of single agent cetuximab in patients with persistent or recurrent epithelial ovarian or primary peritoneal carcinoma with the potential for dose escalation to rash. *Gynecol. Oncol.*, **113**, 21–27.
11. Behbakht,K. *et al.* (2011) Phase II trial of the mTOR inhibitor, temsirolimus and evaluation of circulating tumor cells and tumor biomarkers in persistent and recurrent epithelial ovarian and primary peritoneal malignancies: a Gynecologic Oncology Group study. *Gynecol. Oncol.*, **123**, 19–26.
12. Ferraro,E. *et al.* (2008) Apoptosome-deficient cells lose cytochrome c through proteasomal degradation but survive by autophagy-dependent glycolysis. *Mol. Biol. Cell*, **19**, 3576–3588.
13. Lum,J.J. *et al.* (2005) Growth factor regulation of autophagy and cell survival in the absence of apoptosis. *Cell*, **120**, 237–248.
14. Boya,P. *et al.* (2005) Inhibition of macroautophagy triggers apoptosis. *Mol. Cell. Biol.*, **25**, 1025–1040.
15. Degtyarev,M. *et al.* (2008) Akt inhibition promotes autophagy and sensitizes PTEN-null tumors to lysosomotropic agents. *J. Cell Biol.*, **183**, 101–116.
16. Cao,C. *et al.* (2006) Inhibition of mammalian target of rapamycin or apoptotic pathway induces autophagy and radiosensitizes PTEN null prostate cancer cells. *Cancer Res.*, **66**, 10040–10047.
17. Katayama,M. *et al.* (2007) DNA damaging agent-induced autophagy produces a cytoprotective adenosine triphosphate surge in malignant glioma cells. *Cell Death Differ.*, **14**, 548–558.
18. Amaravadi,R.K. *et al.* (2007) Autophagy inhibition enhances therapy-induced apoptosis in a Myc-induced model of lymphoma. *J. Clin. Invest.*, **117**, 326–336.
19. Abedin,M.J. *et al.* (2007) Autophagy delays apoptotic death in breast cancer cells following DNA damage. *Cell Death Differ.*, **14**, 500–510.
20. Kipps,E. *et al.* (2013) Meeting the challenge of ascites in ovarian cancer: new avenues for therapy and research. *Nat. Rev. Cancer*, **13**, 273–282.
21. Correa,R.J. *et al.* (2012) Modulation of AKT activity is associated with reversible dormancy in ascites-derived epithelial ovarian cancer spheroids. *Carcinogenesis*, **33**, 49–58.
22. Burleson,K.M. *et al.* (2004) Ovarian carcinoma ascites spheroids adhere to extracellular matrix components and mesothelial cell monolayers. *Gynecol. Oncol.*, **93**, 170–181.
23. Allen,H.J. *et al.* (1987) Isolation and morphologic characterization of human ovarian carcinoma cell clusters present in effusions. *Exp. Cell Biol.*, **55**, 194–208.
24. Iwanicki,M.P. *et al.* (2011) Ovarian cancer spheroids use myosin-generated force to clear the mesothelium. *Cancer Discov.*, **1**, 144–157.
25. Shield,K. *et al.* (2009) Multicellular spheroids in ovarian cancer metastases: Biology and pathology. *Gynecol. Oncol.*, **113**, 143–148.

26. Shepherd,T.G. *et al.* (2006) Primary culture of ovarian surface epithelial cells and ascites-derived ovarian cancer cells from patients. *Nat. Protoc*., **1**, 2643–2649.
27. Taylor-Harding,B. *et al.* (2010) Fluvastatin and cisplatin demonstrate synergistic cytotoxicity in epithelial ovarian cancer cells. *Gynecol. Oncol*., **119**, 549–556.
28. Manning,B.D. *et al.* (2007) AKT/PKB signaling: navigating downstream. *Cell*, **129**, 1261–1274.
29. Calleja,V. *et al.* (2009) Role of a novel PH-kinase domain interface in PKB/Akt regulation: structural mechanism for allosteric inhibition. *PLoS Biol*., **7**, e17.
30. Sarbassov,D.D. *et al.* (2005) Phosphorylation and regulation of Akt/PKB by the rictor-mTOR complex. *Science*, **307**, 1098–1101.
31. Choi,A.M. *et al.* (2013) Autophagy in human health and disease. *N. Engl. J. Med*., **368**, 651–662.
32. Mizushima,N. *et al.* (2010) Methods in mammalian autophagy research. *Cell*, **140**, 313–326.
33. Hu,C. *et al.* (2008) The efficacy and selectivity of tumor cell killing by Akt inhibitors are substantially increased by chloroquine. *Bioorg. Med. Chem*., **16**, 7888–7893.
34. Liu,J. *et al.* (2011) Beclin1 controls the levels of p53 by regulating the deubiquitination activity of USP10 and USP13. *Cell*, **147**, 223–234.
35. Burleson,K.M. *et al.* (2004) Ovarian carcinoma spheroids disaggregate on type I collagen and invade live human mesothelial cell monolayers. *Clin. Exp. Metastasis*, **21**, 685–697.
36. Chou,T.C. *et al.* (1984) Quantitative analysis of dose-effect relationships: the combined effects of multiple drugs or enzyme inhibitors. *Adv. Enzyme Regul*., **22**, 27–55.
37. White,E. *et al.* (2009) The double-edged sword of autophagy modulation in cancer. *Clin. Cancer Res*., **15**, 5308–5316.
38. Lu,Z. *et al.* (2008) The tumor suppressor gene ARHI regulates autophagy and tumor dormancy in human ovarian cancer cells. *J. Clin. Invest*., **118**, 3917–3929.
39. Degenhardt,K. *et al.* (2006) Autophagy promotes tumor cell survival and restricts necrosis, inflammation, and tumorigenesis. *Cancer Cell*, **10**, 51–64.
40. Hamilton,G. (1998) Multicellular spheroids as an *in vitro* tumor model. *Cancer Lett*., **131**, 29–34.
41. Tang,M.K. *et al.* (2010) c-Met overexpression contributes to the acquired apoptotic resistance of nonadherent ovarian cancer cells through a cross talk mediated by phosphatidylinositol 3-kinase and extracellular signal-regulated kinase ½. *Neoplasia*, **12**, 128–138.
42. Yoshida,Y. *et al.* (2008) Laminin-1-derived scrambled peptide AG73T disaggregates laminin-1-induced ovarian cancer cell spheroids and improves the efficacy of cisplatin. *Int. J. Oncol*., **32**, 673–681.
43. Xing,H. *et al.* (2007) Knock-down of P-glycoprotein reverses taxol resistance in ovarian cancer multicellular spheroids. *Oncol. Rep*., **17**, 117–122.
44. Xing,H. *et al.* (2005) Effect of the cyclin-dependent kinases inhibitor p27 on resistance of ovarian cancer multicellular spheroids to anticancer chemotherapy. *J. Cancer Res. Clin. Oncol*., **131**, 511–519.
45. Green,S.K. *et al.* (2004) Antiadhesive antibodies targeting E-cadherin sensitize multicellular tumor spheroids to chemotherapy *in vitro*. *Mol. Cancer Ther*., **3**, 149–159.
46. Sotelo,J. *et al.* (2006) Adding chloroquine to conventional treatment for glioblastoma multiforme: a randomized, double-blind, placebo-controlled trial. *Ann. Intern. Med*., **144**, 337–343.
47. Briceño,E. *et al.* (2003) Therapy of glioblastoma multiforme improved by the antimutagenic chloroquine. *Neurosurg. Focus*, **14**, e3.
48. McAfee,Q. *et al.* (2012) Autophagy inhibitor Lys05 has single-agent antitumor activity and reproduces the phenotype of a genetic autophagy deficiency. *Proc. Natl. Acad. Sci. U. S. A*., **109**, 8253–8258.
49. Salabei,J.K. *et al.* (2013) PDGF-mediated autophagy regulates vascular smooth muscle cell phenotype and resistance to oxidative stress. *Biochem. J*., **451**, 375–388.
50. Vakifahmetoglu-Norberg,H. *et al.* (2013) Chaperone-mediated autophagy degrades mutant p53. *Genes Dev*., **27**, 1718–1730.

Received October 16, 2013; revised January 21, 2014; accepted February 14, 2014